

A Low-Profile Wideband Metasurface Antenna With Fan-Beam Radiation

XUE REN^{1,2,3} (Member, IEEE), YOUNG BAO^{1,2,3}, ZEHAI WU⁴, QUAN-WEI LIN⁵ (Member, IEEE),
AND HANG WONG⁵ (Senior Member, IEEE)

¹College of Electronics and Information Engineering, Shenzhen University, Shenzhen 518060, China

²Institute of Microelectronics, Shenzhen University, Shenzhen 518060, China

³Guangdong Provincial Key Laboratory of Millimeter-Wave and Terahertz, South China University of Technology, Guangzhou 510641, China

⁴R&D Center, Broadradio Communication Technology Company Ltd., Guangzhou 510530, China

⁵State Key Laboratory of Terahertz and Millimeter Waves, Department of Electrical Engineering, City University of Hong Kong, Hong Kong, SAR, China

CORRESPONDING AUTHOR: H. WONG (e-mail: hang.wong@cityu.edu.hk)

This work was supported in part by the Guangdong Provincial Key Laboratory of Millimeter-Wave and Terahertz under Grant 2019B030301002KF2103; in part by the Research Grants Council of the Hong Kong SAR, China, under Project CRF CityU C1020-19E; in part by the Guangdong Provincial Department of Science and Technology, China, under Project 2020B1212030002; in part by the Guangdong-Hong Kong Technology Cooperation Funding Scheme under Grant 2021A0505110006; and in part by the Shenzhen Science and Technology Program under Grant KQTD20200820113046084.

ABSTRACT This work presents a design of a fan-beam metasurface with a low profile and a wide operating bandwidth. We introduce a new meta unit of four-loop structure which produces high refractive index over the wide operating bandwidth. The metasurface composes of impedance matching layers and core layers to contribute to the fan-beam radiation. A prototype working at X-band is designed, fabricated, and measured. The measured results agree well with simulated ones. The measured results exhibit a wide bandwidth of 51%. The measured fan-beam radiation performances show that the 3-dB beamwidths on E and H-plane are 17° and 45°, respectively. The realized metasurface is with the height of about 0.24 λ_0 , where λ_0 is the wavelength at center frequency in free space. Measured realized gain is about 15.6 dBi at center frequency. In addition, the measured cross polarization discrimination is better than 25 dB across the entire bandwidth.

INDEX TERMS Broadband, metasurface, gradient refractive index (GRIN), lens antenna, fan-beam.

I. INTRODUCTION

FAN-BEAM antennas are popularly used in imaging systems and remote sensing satellite communication systems. The radiation features of this type of the antennas with narrow beam width on one principal plane and wide beam width on the orthogonal plane [1]–[6]. Lenses are one of the good approaches applying to the design of fan-beam antennas due to the ease of producing wide operating bandwidths, directive radiation beam, and high capability in linear and circular polarization to the antennas. Conventionally, the lenses can be designed with dielectric materials as planar hyperbolic or planar spherical and slotted structure which is able to focus the radiation beam to the assigned direction with high directivity and high gain [7]–[8]. However, the dielectric lenses are bulky to meet miniaturization and

integration development requirements for recent electronic systems. Recently, planar lens developments by the use of metamaterials propose to solve bulky problem of the lens by metalenses, metasurfaces, and metareflectors, which can achieve the manipulation of controls of the electromagnetic waves.

According to the property of the metamaterials, the metamaterial antennas can be classified into the negative index metamaterial (NIM) [9]–[12], zero-index metamaterial (ZIM) [13], and gradient refractive index (GRIN) [14]–[15]. Gradient refractive index metamaterial-based lens or metasurfaces [16]–[24] features with advantages of wide bandwidth and low profile. Therefore, it has attracted many attentions to design this novel metamaterial lens. Especially, this type lens or metasurface shows wideband performance

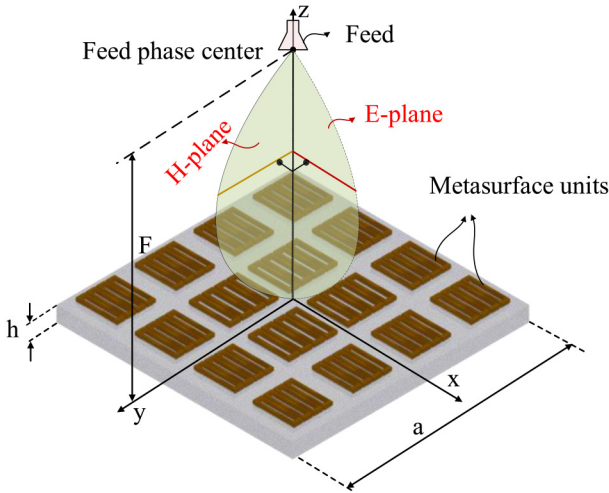


FIGURE 1. Configuration of a metasurface lens antenna.

compare with low/zero-index or negative index metamaterial-based designs [25]–[27]. In [17], a collapsible metamaterial lens antenna was developed with high gain performance by using the GRIN unit cell. The air gap between adjacent dielectric layers enables the collapsible deployment. The lens is with height of $0.92 \lambda_0$ in operational arrangement, where λ_0 is the wavelength of its operating frequency at 13.4 GHz. In [22], a low-profile and wideband lens antenna based on metasurface has been proposed to realize high gain performance at X band. However, the above examples of metalenses and metasurfaces have not given a solution for producing fan-beam radiation from the antenna except [15], in which three different kinds of substrate materials were used to cover the requirement refractive index range.

In this paper, a GRIN metamaterial unit cell composed of four rectangular metal loops with large refractive index variation is proposed to build core layers (CLs) and impedance matching layers (IMLs) for the multilayer metasurface. The transmission characteristic of the proposed unit cell is carried out and analyzed. A wideband and low-profile metasurface is developed based on the proposed unit cell. The measured reflection coefficient is lower than -10 dB from 7.35 to 12.35 GHz. The fan-beam radiation is realized successfully. By utilizing the IML, the profile of lens is further reduced and the peak aperture efficiency reaches up to 60%. The final profile is about $0.24\lambda_0$, where λ_0 is the wavelength at center frequency in free space. The measured gain is 15.4 dBi at the center frequency of 10 GHz and it can reach up to 16.4 dBi within the operating bandwidth.

II. METASURFACE LENS ANTENNA DESIGN

Fig. 1 schematically shows the configuration of the proposed metasurface lens antenna. This lens antenna consists of a planar circular metasurface which includes both impedance matching layers and core layers. A horn located centrally at

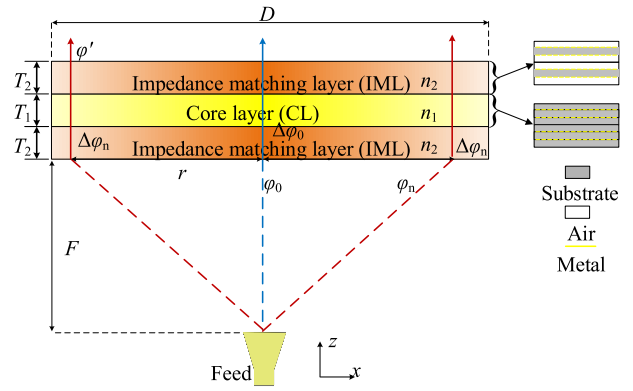


FIGURE 2. Schematic of a GRIN lens antenna.

the focal point of the metasurface is used to excite electromagnetic wave to illuminate the proposed metasurface lens antenna. The metasurface is composed of a set of period unit cells with different refractive indexes varying across the lens aperture. In order to achieve a high-gain characteristic, the unit cells must be designed to compensate the different phase delay of the incident wave illuminated from the phase center of the feed and arrived on the center of the unit cells with respect to the ray passing through the center of the lens aperture in order to obtain a highly directional radiation pattern on certain plane. From the configuration of the lens, the compensation can be achieved through changing the geometrical dimensions of metallic pattern in the surface of the unit cells across the lens aperture.

The schematic of the metasurface antenna is shown in Fig. 2. The metasurface is normally excited by the wideband source antenna (the feed) with proper focal to diameter ratio. The proposed metasurface is composed of two CLs and two IMLs located on both sides of the CL. In order to improve the transmission efficiency, the height of the IML is set about a quarter wavelength. And the height of the CL and IMLs can be determined by [22]

$$2T_2n_2(r) + T_1n_1(r) = Tn(r) \quad (1)$$

where T_1 , T_2 are the height of the CLs and IMLs, and the $n_1(r)$, $n_2(r)$ are the refractive index at the same x -direction of the CL and IMLs as shown in the Fig 2, r is the distance between the unit cell and the center point of lens, F denotes the focal length of lens. T and $n(r)$ are the thickness and refractive index for the lens without IMLs. The refractive index value of the IMLs is the square root of the CL for impedance matching. So, the refractive index value of the CL is larger than that of IMLs. And the refractive index should be gradually faded from the center to the edge to compensate the phase difference for spherical incident waves on different part of metasurface. The phase difference phenomenon is also shown in Fig. 2. The deep color represents higher refractive index value, and light color in the marginal region means smaller value of refractive index.

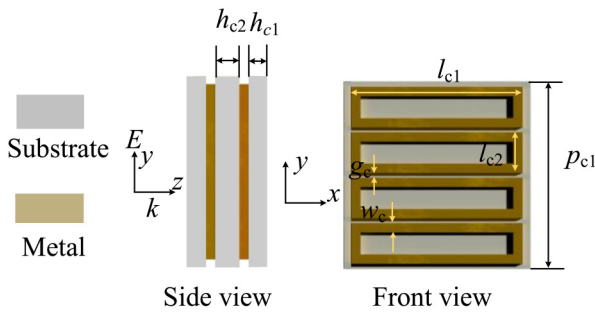


FIGURE 3. Structure of the CLs unit cell.

The wave reaches the metasurface with different phase range from φ_0 to φ_n . After passing the proposed metasurface, the phase distribution is expected to be modulated with same value on the aperture of metasurface. As a result, if a fan beam antenna is designed with narrower E-plane beam, the equivalent refractive index value of CL should vary along with E-plane direction, while the refractive index distribution on the orthogonal direction remains unchanged. The detailed design process of the unit cell of IMLs and CLs are described in the following sections.

A. UNIT CELL DESIGN OF THE CL

Fig. 3 shows the detailed structure of the proposed CL unit cell. The unit cell here is based on three substrate layers with same material, and two metal layers printed between the substrates. The metal layer consists of four rectangular metal loops. The substrate used is *Rogers RO4350B* with the dielectric constant of 3.48. The height of the middle layer of the unit cell is 0.508mm. Top and bottom layers of the substrate are with the height of 0.254mm. When the unit cell is excited with a normally incident wave propagating in the z -direction and its electric field along with the long side of rectangular metal strip, the incident electric field induces charge displacement on the bilayer metal pattern of the unit cell [10]. Thus, capacitance is created between the upper and bottom of the metal pattern. The increasing of the size will lead to a strong capacitive coupling effect which can be used to vary the equivalent refractive index of the unit cell into desirable values of the refractive index of the metasurface, which will show in following explanation. The unit cell is excited with the longer strips parallel with the direction of the incident electric field. The simulated reflection coefficient and transmission responses are shown in Fig. 4 under $p_{c1} = 4$ mm, $l_{c1} = 3.7$ mm, $l_{c2} = 0.87$ mm, $g_c = 0.1$ mm, $w_c = 0.2$ mm. It can be observed that the resonant frequency is located at about 16.4 GHz. The equivalent refractive index value of the CL unit cell is extracted and shown in Fig. 4. The results depict that the real part of the unit cell's equivalent refractive index value is high and stable within wide bandwidth from 5 to 15 GHz. In addition, the imaginary part of refractive index is very close to zero, which indicates low losses in the same wide bandwidth.

From the study of simulation, it was found that the metal strip with the length l_{c1} is related to the refractive index.

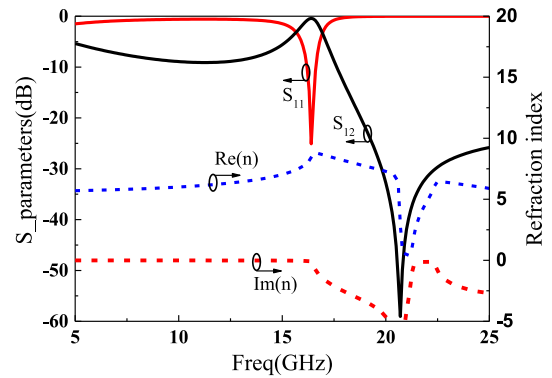


FIGURE 4. Extracted equivalent refractive index performance of the core layer unit cell.

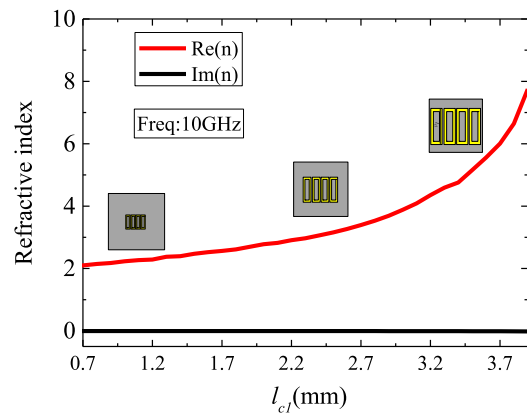


FIGURE 5. Refractive index variation of CL unit cell with different values of l_{c1} .

Fig. 5 shows the refractive index variation with the different length l_{c1} from 0.5 to 3.9mm at 10 GHz. The refractive index varies from 2 to 7.75 as shown in Fig. 5, and the larger l_{c1} leads to the increasing of the real part of the refractive index. The simulation result agrees well with the theoretical analysis in the preceding paragraph. Meanwhile, the imaginary part of the refractive index is stably and close to zero over the whole frequency bands. It can be observed that the proposed unit cell shows wide variation range (5.75) for the real part of refractive index. The large real part variation of refractive index is what we need to design low profile metasurface antenna.

It can be observed from Fig. 2 that the unit cells at edge part of the lens are with small refractive index value and will be excited by the oblique incidence. Thus, the investigation of the CL layer with $l_{c1} = 2$ mm under 45-degree incidence is carried out. Fig. 6 shows the S -parameter performance and equivalent refractive index of the unit cell. It can be observed that the refractive index is stable in wide bandwidth, which indicates that the it is still suitable for wideband application.

B. UNIT CELL DESIGN OF THE IML

Fig. 7 shows the configuration of the unit in IMLs. The main structure of IML unit cell is the same as that of CL. The substrate here is the same with that in CL unit cell design.

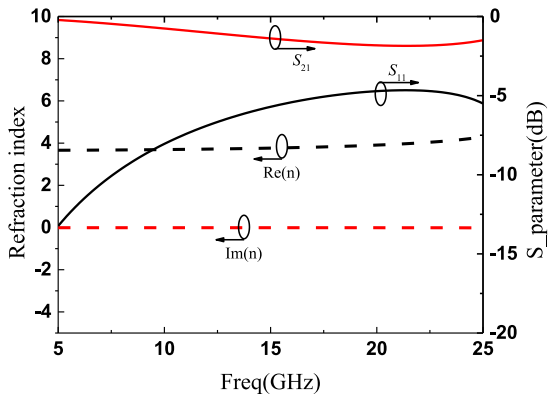


FIGURE 6. S-parameter and equivalent refractive index performance of the CL unit cell with $l_{c1} = 2$ mm under 45-degree oblique incidences.

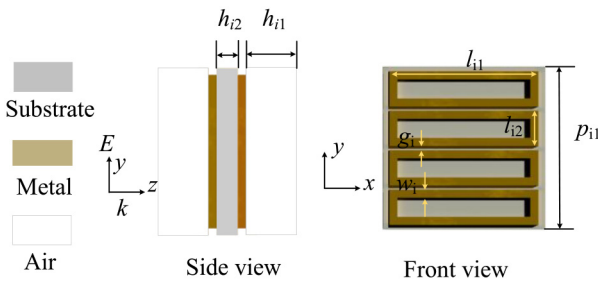


FIGURE 7. Structure of the IMLs unit cell.

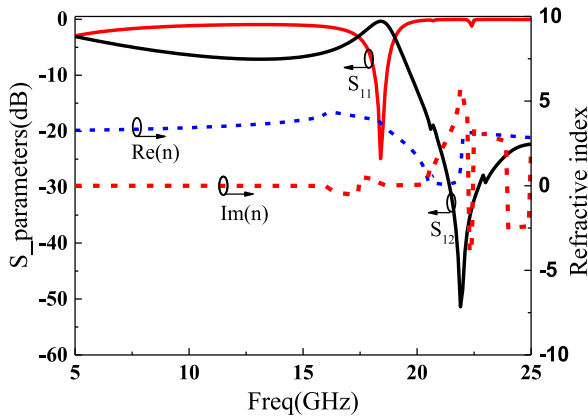


FIGURE 8. Extracted equivalent refractive index performance of the IMLs unit cell.

The difference is that the top and bottom thin substrate layers are replaced with air in the impedance matching unit cell. The proposed unit cell is also excited by normally incident wave with the direction of electric field parallel the longer strip of metal strips. Similar with the CL unit cell, the transmission characteristic and equivalent refractive index performance analysis is carried out. Fig. 8 shows the S-parameters response and the extracted refractive index of the IMLs unit cell with $p_{i1} = 4$ mm, $l_{i1} = 3.7$ mm, $l_{i2} = 0.87$ mm, $g_i = 0.1$ mm, $w_i = 0.2$ mm, $h_{i1} = 0.8$ mm, $h_{i2} = 0.508$ mm. It can be observed that the resonant frequency is located at about 18.4 GHz. It also depicts that the unit

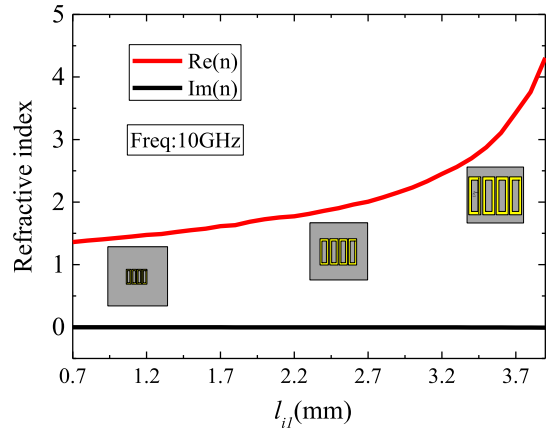


FIGURE 9. Refractive index variation of IMLs unit cell with different values of l_{i1} .

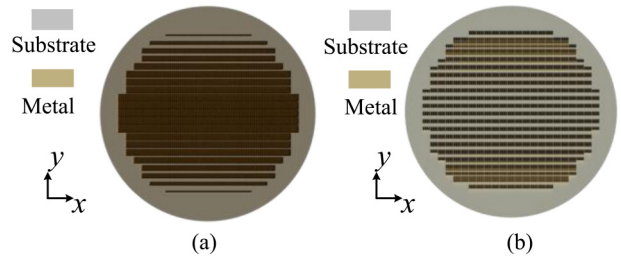


FIGURE 10. Patterns of the metallic strip on (a) CLs and (b) IMLs.

cell presents stable refractive index value within the wide bandwidth from 5 to 15 GHz. In the design, the refractive index of the IMLs unit cell is about the geometrical mean of the CL for impedance matching. Therefore, a large refractive index variation range is also expected. Like the CL unit cell, the refractive index variation with the different length l_{i1} from 0.5 mm to 3.9 mm at 10 GHz is investigated. In Fig. 9, it is depicted that the real part variation range of refractive index is from 1.36 to 4.3, and the larger l_{i1} leads to the increasing of the real part of the refractive index. Meanwhile, the imaginary part of the refractive index is stably and close to zero over the whole frequency bands. It can be observed that the proposed unit cell for IML design is also shows wide variation range of refractive index and suitable for IML application.

III. RESULTS AND DISCUSSION

To verify the working principle, a prototype was designed and fabricated. To realize the expected phase response and good transmission performance, the IML is constructed by two stacked IMLs. Additionally, the CL also designed with same layers, as shown in Fig. 2. Fig. 10 shows the patterns of the metallic strips for the CLs and IMLs. The substrate used is Rogers 4350B. The photography of the fabricated antenna is shown in Fig. 11. The multilayer substrates are aligned and tied together by using nylon screws. The measurement setup is depicted in Fig. 12. The feed is based on our previous design in [22]. The part of metasurface is about $3.06 \lambda_0$. The

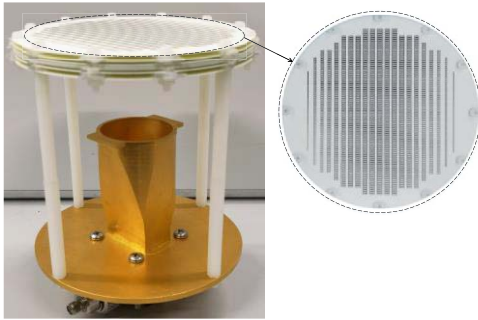


FIGURE 11. Photography of the fabricated antenna.

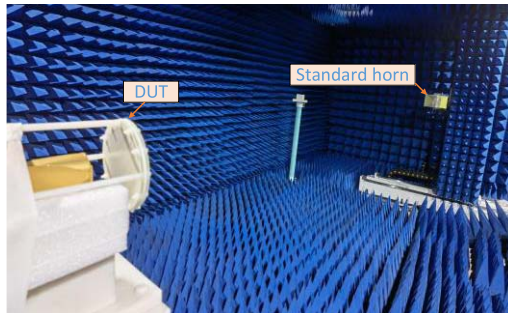


FIGURE 12. Measurement set up in microwave anechoic chamber.

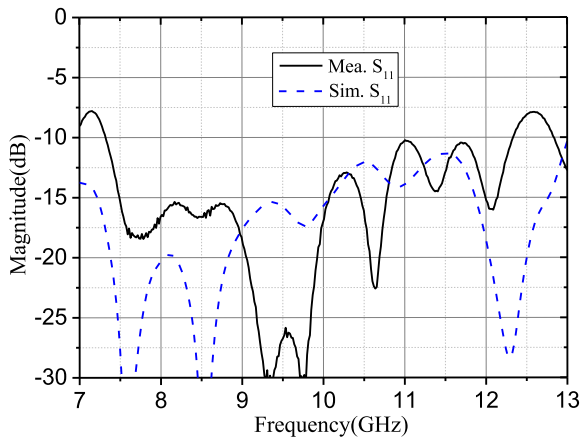


FIGURE 13. Simulated and measured results of the reflection coefficient.

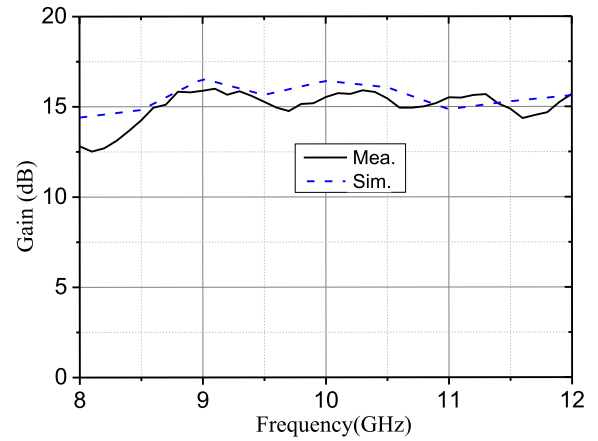


FIGURE 14. Simulated and measured boresight gain performance of the fabricated prototype.

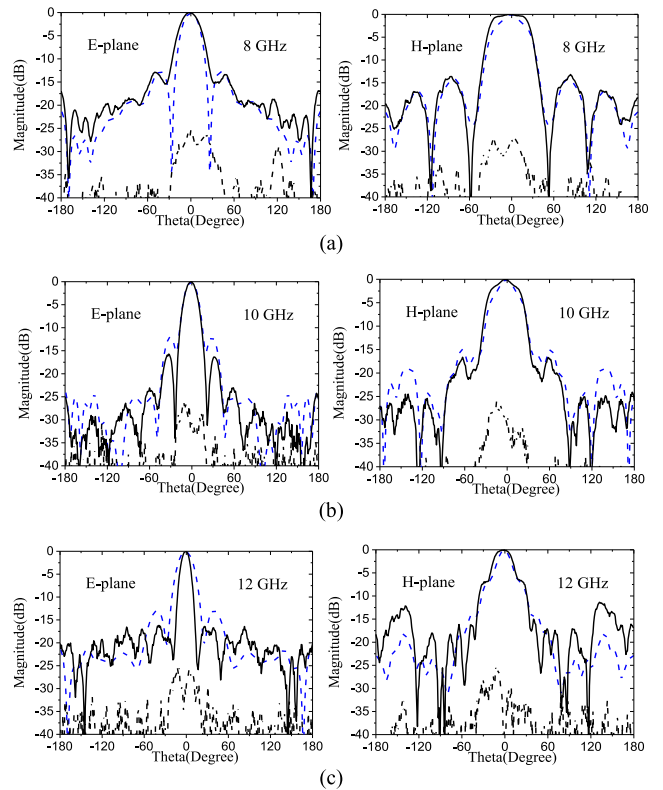


FIGURE 15. Simulated and measured radiation patterns on two principal planes at (a) 8, (b) 10 and (c) 12 GHz.

final focal length to metasurface diameter ratio is set about 0.4. Fig. 13 shows the simulated and measured results of the reflection coefficient. The antenna's working frequency is at X band. It shows that the reflection magnitude is less than -10 dB from about 7.35 to 12.35 GHz. The simulated and measured results of the boresight gain is depicted in Fig. 14. The measured boresight gain varies from 12.5 to 16 dBi. The gain is greater 14.5 dB from 8.55 to 12 GHz.

Simulated and measured radiation patterns at 8, 10 and 12 GHz are shown in Fig. 15. The 3-dB beamwidths of the E-plane are 28° , 17° , and 13° at 8, 10 and 12 GHz, respectively. In the H-plane, the corresponding 3-dB beamwidths are 58° , 45° , and 30° . It can be observed that the fan-beam

radiation is realized while the beamwidth of the radiation pattern at the E-plane is narrower than that of the H-plane. In addition, the measured cross-polarization is lower than 25 dB within the whole operating bandwidth. According to the measure results, the obtained aperture efficiencies of the proposed antenna is over 43.3% at the center frequency of 10 GHz and can reach up to about 60% at 8.8 GHz. The

TABLE 1. Comparison of proposed design with previous works.

Ref.	CF ^a (GHz)	profile (λ_0)	Technology	RG ^b	RRI ^c	RT ^d
[5]	30	0.68	Luneberg lens	17.7	1.54	Fan-beam (endfire)
[6]	60	0.88	Luneberg lens	-	-	Fan-beam (endfire)
[15]	10	0.5	GRIN Meta-lens	17.7	>1.6 ^e	Fan-beam (endfire)
[22]	10	0.26	GRIN Meta-lens	-	4.76	Pencil-beam (boresight)
[24]	10	0.27	GRIN Meta-lens	11.1	3.03	Fan-beam (endfire)
This work	10	0.24	GRIN Meta-lens	15.6	5.75	Fan-beam (boresight)

^aCF: center frequency; ^bRG: realized gain; ^cRRI: range of refractive index; ^dRT: radiation type; ^e: three kinds of materials used in the design.

lens height is about $0.24 \lambda_0$, where λ_0 is the wavelength of 10 GHz in free space. The measured results agree well with the simulated ones, which confirmed the design principle of the proposed lens antenna. The difference between the measured and simulated results may due to the error during the metasurface fabrication and fixture assembly process.

The comparison between the propose design with previous works is shown in Table 1. It can be observed that the proposed metasurface shows low profile by using the GRIN technology. Besides, the developed unit cell draws large variation range of refractive index, which is beneficial for low profile lens design. The comparison table also shows that most of the previous lens-based fan-beam antenna feature with endfire radiation. The proposed design draws boresight fan-beam radiation characteristic.

IV. CONCLUSION

A wideband and thin-profile metasurface was introduced to produce fan-beam radiation over a wide operating bandwidth. Both CL and IML unit cell of the metasurface were discussed. The proposed meta unit has a merit in contributing a large refractive index and a thin cross-sectional structure over the operating bandwidth. The final height of the metasurface is about $0.24 \lambda_0$, where λ_0 is the wavelength of 10 GHz in free space. The proposed antenna shows an excellent fan-beam performance with a desirable gain of 15.5 dBi. This proposed metasurface antenna technology finds potential application in satellite communications and sensing networks.

REFERENCES

- [1] J. Huang and Y. Rahmat-Samii, "Fan beam generated by a linear-array fed parabolic reflector," *IEEE Trans. Antennas Propag.*, vol. 38, no. 7, pp. 1046–1053, Jul. 1990.
- [2] M. Ye, X.-R. Li, and Q.-X. Chu, "Single-layer circularly polarized antenna with fan-beam endfire radiation," *IEEE Antennas Wireless Propag. Lett.*, vol. 16, pp. 20–23, 2017.
- [3] H. Lee, Y. H. Kim, V. A. Volkov, R. V. Kozhin, D. M. Vavriv, and T. S. Lim, "35 GHz compact radar using fan beam antenna array for obstacle detection," *Electron. Lett.*, vol. 43, no. 25, pp. 1641–1642, Dec. 2007.
- [4] H. Nakano, M. Iwatsuki, M. Sakurai, and J. Yamauchi, "A cavity-backed rectangular aperture antenna with application to a tilted fan beam array antenna," *IEEE Trans. Antennas Propag.*, vol. 51, no. 4, pp. 712–718, Apr. 2003.
- [5] X. Wu and J.-J. Laurin, "Fan-beam millimeter-wave antenna design based on the cylindrical Luneberg lens," *IEEE Trans. Antennas Propag.*, vol. 55, no. 8, pp. 2147–2156, Aug. 2007.
- [6] Z. Zhang, S. Yang, Y. Chen, S. Qu, and J. Hu, "Fast analysis of parallelplate cylindrical Luneberg lens antennas through Dyadic Green's fuctions," *IEEE Trans. Microw. Theory Techn.*, vol. 66, no. 10, pp. 4327–4337, Oct. 2018.
- [7] H. D. Hristov and J. M. Rodriguez, "Design equation for multielectric fresnel zone plate lens," *IEEE Microw. Wireless Compon. Lett.*, vol. 22, no. 11, pp. 574–576, Nov. 2012.
- [8] D. N. Black and J. C. Wiltse, "Millimeter-wave characteristics of phase-correcting fresnel zone plates," *IEEE Trans. Microw. Theory Techn.*, vol. MTT-35, no. 12, pp. 1122–1129, Dec. 1987.
- [9] A. K. Iyer and G. V. Eleftheriades, "A multilayer negative-refractive-index transmission-line (NRI-TL) metamaterial free-space lens at X-band," *IEEE Trans. Antennas Propag.*, vol. 55, no. 10, pp. 2746–2753, Oct. 2007.
- [10] S. N. Burokur, A. Sellier, B. Kanté, and A. de Lustrac, "Symmetry breaking in metallic cut wire pairs metamaterials for negative refractive index," *Appl. Phys. Lett.*, vol. 94, pp. 1–3, May 2009.
- [11] M. Navarro-Cia, M. Beruete, I. Campillo, and M. S. Ayzá, "Beamforming by left-handed extraordinary transmission metamaterial bi- and plano-concave lens at millimeter-waves," *IEEE Trans. Antennas Propag.*, vol. 59, no. 6, pp. 2141–2151, Jun. 2011.
- [12] S. Das, H.-L. Nguyen, G. N. Babu, and A. K. Iyer, "Free-space focusing at C-band using a flat fully printed multilayer metamaterial lens," *IEEE Trans. Antennas Propag.*, vol. 63, no. 11, pp. 4702–4714, Nov. 2015.
- [13] L. H. Yuan, W. X. Tang, H. Li, Q. Cheng, and T. J. Cui, "Three-dimensional anisotropic zero-index lenses," *IEEE Trans. Antennas Propag.*, vol. 62, no. 8, pp. 4135–4142, Aug. 2014.
- [14] Z. L. Mei, J. Bai, T. M. Niu, and T. J. Cui, "A half maxwell fish-eye lens antenna based on gradient-index metamaterials," *IEEE Trans. Antennas Propag.*, vol. 60, no. 1, pp. 398–401, Jan. 2012.
- [15] N. Zhang, W. X. Jiang, H. F. Ma, W. X. Tang, and T. J. Cui, "Compact high-performance lens antenna based on impedance-matching gradient-index metamaterial," *IEEE Trans. Antennas Propag.*, vol. 67, no. 2, pp. 1323–1328, Feb. 2019.
- [16] X. Q. Lin, T. J. Cui, J. Y. Chin, X. M. Yang, and R. Liu, "Controlling electromagnetic waves using tunable gradient dielectric metamaterial lens," *Appl. Phys. Lett.*, vol. 92, pp. 1–3, Apr. 2008.
- [17] A. papathanasopoulos, Y. Rahmat-Samii, N. C. Garcia, and J. D. Chisum, "A novel collapsible flat-layered metamaterial gradient-refractive-index lens antenna," *IEEE Trans. Antennas Propag.*, vol. 68, no. 3, pp. 1312–1321, Mar. 2020.
- [18] E. Erfani, M. Niroo-Jazi, and S. Tatu, "A high-gain broadband gradient refractive index metasurface lens antenna," *IEEE Trans. Antennas Propag.*, vol. 64, no. 5, pp. 1968–1973, May 2016.
- [19] R. Liu, Q. Cheng, J. Y. Chin, J. J. Mock, T. J. Cui, and D. R. Smith, "Broadband gradient index microwave quasi-optical elements based on non-resonant metamaterials," *Opt. Exp.*, vol. 17, no. 23, pp. 21030–21041, Nov. 2009.
- [20] M. Q. Qi *et al.*, "Suppressing side-lobe radiations of horn antenna by loading metamaterial lens," *Sci. Rep.*, vol. 5, p. 9113, Nov. 2015.
- [21] A. Dadgarpour, B. Zarghooni, B. S. Virdee, and T. A. Denidni, "Beam-deflection using gradient refractive-index media for 60-GHz end-fire antenan," *IEEE Trans. Antennas Propag.*, vol. 63, no. 8, pp. 3768–3774, Aug. 2015.
- [22] Q.-W. Lin and H. Wong, "A low-profile and wideband lens antenna based on high-refractive-index metasurface," *IEEE Trans. Antennas Propag.*, vol. 66, no. 11, pp. 5764–5772, Nov. 2018.

- [23] H. F. Ma, B. G. Cai, T. X. Zhang, Y. Yang, W. X. Jiang, and T. J. Cui, "Three-dimensional gradient-index materials and their applications in microwave lens antennas," *IEEE Trans. Antennas Propag.*, vol. 61, no. 5, pp. 2561–2569, May 2013.
- [24] X. Ren, Q.-W. Lin, H. Wong, and W. He, "A compact gradient refractive index metamaterial lens for endfire fan-beam radiation," *IEEE Antennas Wireless Propag. Lett.*, vol. 20, no. 12, pp. 2339–2343, Dec. 2021.
- [25] T. Sriscoll *et al.*, "Free-space microwave focusing by a negative-index gradient lens," *Appl. Phys. Lett.*, vol. 88, pp. 1–3, Feb. 2006.
- [26] Z. G. Xiao and H. L. Xu, "Low refractive MTMs for gain enhancement of horn antenna," *J. Infrared Mil. Terahertz Waves*, vol. 30, no. 3, pp. 225–232, 2009.
- [27] H. Xu, G. Wang, and T. Cai, "Miniaturization of 3-D anisotropic zero refractive-index metamaterials with application to directive emissions," *IEEE Trans. Antennas Propag.*, vol. 62, no. 6, pp. 3141–3149, Jun. 2014.



XUE REN (Member, IEEE) received the Ph.D. degree in electrical engineering from the State Key Laboratory of Terahertz and Millimeter Waves, City University of Hong Kong (CityU), Hong Kong, in 2020.

In 2020, he joined Shenzhen Tongxian Technology Company Ltd., Shenzhen, China, as a Senior Antenna Engineer. From 2015 to 2016, he was a Research Assistant with the Shenzhen Key Laboratory of MWWC, Shenzhen Research Institute, City University of Hong Kong,

Shenzhen. He is currently an Assistant Professor with the College of Electronics and Information Engineering, Shenzhen University, Shenzhen. His current research interests include beamforming antennas, satellite antennas, metamaterials, millimeter-wave antennas, array technology, and RF front-end circuits. He was a recipient of the Outstanding Academic Performance Award from CityU in 2018 and 2019. He also serves as a Reviewer for several technique journals, including *IEEE TRANSACTIONS ON ANTENNAS AND PROPAGATION* and the *IEEE ANTENNAS AND WIRELESS PROPAGATION LETTERS*. He was a TPC Member of the Cross Strait Radio Science and Wireless Technology Conference 2021, Shenzhen, and the IEEE MTT-S International Microwave Workshop Series on Advanced Materials and Processes for RF and THz Applications in 2022.



YOUPENG BAO was born in Jiangxi, China. He received the B.S. degree in telecommunications engineering from Nanchang University, Nanchang, China, in 2021. He is currently pursuing the M.S. degree in communication and information with the South China University of Technology, Guangzhou, China.

His research interests include lens antennas, metasurface antennas, millimeter-wave antennas, deep learning, and microwave theory.



ZEHAI WU was born in Jingzhou, China. He received the B.S. degree in information engineering and the M.S. degree in communication and information systems from the South China University of Technology (SCUT), Guangzhou, China, in 2002 and 2005, respectively, and the Ph.D. degree from the City University of Hong Kong, Hong Kong, in 2010.

He worked as a Research and Development Engineer with Argus Technologies (China) Ltd., Guangzhou, from 2010 to 2013, and focused on multibeam antenna design. He joined newly established Guangdong Broadradio Communication Technology Company Ltd. in 2013, and developed wideband stadium antennas with rectangular coverage, wideband multibeam antennas with low grating lobe, FDD/TDD antennas for 5G mobile communication systems. The antenna products brought high-capacity solutions for European Football Championship 2016, France, and FIFA World Cup 2018 in Russia, and are highly rated for good performance. His current research interests include novel base station antenna for 5G/4G systems.



QUAN-WEI LIN (Member, IEEE) was born in Xinhui, Guangdong, China. He received the B.E. degree in information engineering and the M.E. degree in communication and information systems from South China University of Technology, Guangzhou, China, in 2013 and 2016, respectively, and the Ph.D. degree in electrical engineering from the City University of Hong Kong, Hong Kong, in 2019.

He joined the State Key Laboratory of Terahertz and Millimeter Waves, City University of Hong Kong as a Postdoctoral Fellow in 2019. His current research interests include antennas, metasurface, and microwave rectifier.

Dr. Lin was a recipient of the Third Prize in the Student Innovation Competition of the 2013 IEEE International Workshop on Electromagnetics.



HANG WONG (Senior Member, IEEE) received the B.Eng., M.Phil., and Ph.D. degrees in electronic engineering from the City University of Hong Kong, Hong Kong, in 1999, 2002, and 2006, respectively, where he joined the Department of Electronic Engineering in 2012. He had several visiting professorships with Stanford University, USA, in 2011; University of Waterloo, Canada, in 2013; University of College London, U.K., in 2014; and the University of Limoges, France, in 2015. He is the Director of the Applied

Electromagnetics Laboratory, CityU. He has over 190 publications, two coauthored book chapters, and 20 U.S. and China patents. His achievements led to receiving numerous awards at local, national, and international conferences. For example, he received the Best Paper Award at the National Conference 2017 Les Journées Nationales Microondes, France; the Best Paper Award at the 2017 IEEE International Workshop on Electromagnetics, U.K.; the Best Associate Editor Award 2016 of an *IEEE ANTENNAS AND WIRELESS PROPAGATION LETTERS*, USA; and an Outstanding Scientist Award of 2016 in Shenzhen city presented by Shenzhen Science and Technology Bureau. He was awarded to lead a major project supported by the Ministry of Industry and Information Technology of PRC to develop new antenna elements for TD-LTE and 5G applications. He was the Chair of the IEEE Hong Kong Section of the Antennas and Propagation/Microwave Theory and Techniques Chapter from 2011 to 2014. He was the TPC Co-Chairs of the 10th Global Symposium on Millimeter-Waves, Hong Kong, in 2017, and the IEEE International Workshop on Electromagnetics 2017, London. He was the General Co-Chair of the Asia-Pacific Microwave Conference 2020, Hong Kong, and the General Chair of the Cross Strait Radio Science and Wireless Technology Conference 2021, Shenzhen, China. He is the IEEE APS Region-10 Representative. He is an Associate Editor of *IEEE TRANSACTIONS ON ANTENNAS AND PROPAGATION* and was an Associate Editor of *IEEE ANTENNAS AND WIRELESS PROPAGATION LETTERS*.